Virus-induced gene silencing in the perennial woody *Paeonia ostii*

Lihang Xie Equal first author, , **Qingyu Zhang** Equal first author, , **Daoyang Sun** , **Weizong Yang** , **Jiayuan Hu** , **Lixin Niu** Corresp., , **Yanlong Zhang** Corresp.

Corresponding Authors: Lixin Niu, Yanlong Zhang
Email address: niulixin@nwafu.edu.cn, zhangyanlong@nwafu.edu.cn

Tree peony is a perennial deciduous shrub with great ornamental and medicinal significance. A current limitation for its functional genomic research is the lack of effective molecular genetic tools. Here, the first application of a *Tobacco rattle virus* (TRV)-based virus-induced gene silencing (VIGS) in the tree peony species *P. ostii* is presented. Two different approaches, leaf syringe-infiltration and seedling vacuum-infiltration, were utilized for *Agrobacterium*-mediated infection. The vacuum-infiltration was shown to result in a more complete agrobacterial penetration than syringe-infiltration, and thereby determined as an appropriate inoculation method. The silencing of reporter gene *PoPDS* encoding phytoene desaturase was achieved in TRV-*PoPDS*-infected triennial tree peony plantlets, with a typical photobleaching phenotype shown in uppermost newly-sprouted leaves. The endogenous *PoPDS* transcripts were remarkably down-regulated in VIGS photobleached leaves. Moreover, the green fluorescent protein (GFP) fluorescence was detected in leaves and roots of inoculated plants with TRV-GFP, suggesting the capability of TRV to silence genes in various tissues. Taken together, the data demonstrated that the TRV-based VIGS technique could be adapted for high-throughput functional characterization of genes in tree peony.

Virus-induced gene silencing in the perennial woody *Paeonia ostii*

Lihang Xie† · Qingyu Zhang† · Daoyang Sun† · Weizong Yang · Jiayuan Hu · Lixin Niu* · Yanlong Zhang*

College of Landscape Architecture and Arts, Northwest A&F University, Yangling, Shaanxi 712100, People's Republic of China; Oil Peony Engineering Technology Research Center of National Forestry Administration, Yangling, Shaanxi, People's Republic of China

* To whom correspondence should be addressed:

Lixin Niu

Taicheng Road, Yangling, Shaanxi, 712100, People's Republic of China

Tel: +86-13572582039; Fax: +86-029-87082878; E-mail: niulixin@nwsuaf.edu.cn

Yanlong Zhang

Taicheng Road, Yangling, Shaanxi, 712100, People's Republic of China

Tel: +86-029-87082878; Fax: +86-029-87082878; E-mail: zhangyanlong@nwsuaf.edu.cn

† These authors contributed equally to this work.

Abstract

Tree peony is a perennial deciduous shrub with great ornamental and medicinal significance. A current limitation for its functional genomic research is the lack of effective molecular genetic tools. Here, the first application of a *Tobacco rattle virus* (TRV)-based virus-induced gene silencing (VIGS) in the tree peony species *P. ostii* is presented. Two different approaches, leaf syringe-infiltration and seedling vacuum-infiltration, were utilized for *Agrobacterium*-mediated infection. The vacuum-infiltration was shown to result in a more complete agrobacterial penetration than syringe-infiltration, and thereby determined as an appropriate inoculation method. The silencing of reporter gene *PoPDS* encoding phytoene desaturase was achieved in TRV-*PoPDS*-infected triennial tree peony plantlets, with a typical photobleaching phenotype shown in uppermost newly-sprouted leaves. The endogenous *PoPDS* transcripts were remarkably down-regulated in VIGS photobleached leaves. Moreover, the green fluorescent protein (GFP) fluorescence was detected in leaves and roots of inoculated plants with TRV-GFP, suggesting the capability of TRV to silence genes in various tissues. Taken together, the data demonstrated that the TRV-based VIGS technique could be adapted for high-throughput functional characterization of genes in tree peony.

Keywords *Paeonia ostii*, Virus-induced gene silencing, *Tobacco rattle virus*, *Phytoene desaturase*, Green fluorescent protein

43

44 **Abbreviations**

45	TRV	*Tobacco rattle virus*
46	VIGS	Virus-induced gene silencing
47	PTGS	Post-transcriptional gene silencing
48	PDS	Phytoene desaturase
49	EGFP	Enhanced green fluorescent protein
50	qRT-PCR	Quantitative real-time PCR

51

52 **Introduction**

53 Tree peony is a perennial woody plant belonging to sect. *Moutan* DC. of the genus *Paeonia* L.
54 (Paeoniaceae) (*Li et al., 2009*). It is indigenous to China and the cultivation history can be traced
55 back to 2000 years ago (*Chen & Li, 1998*). As China's unofficial national flower, tree peony has
56 been introduced to Japan, America, Australia, and Europe, with a rise in worldwide popularity. It
57 is commonly known as an ornamental and medicinal crop due to large showy flowers and
58 abundant bioactive substances in roots. Recent reports suggest that the tree peony seed has high
59 yield of oil which contains over 90% unsaturated fatty acids required by human, revealing a
60 tremendous potential of tree peony in future edible oil production (*Wu et al., 2014*). The variety
61 *Paeonia ostii* 'Feng Dan' is a new oil crop widely planted in north China, with its total cultivated
62 area exceeding 16,200 hectares.

For now, a quantity of studies have been carried out on the cloning and functional analysis of genes, associated with flower development (*Li et al., 2016*), bud dormancy (*Zhang et al., 2015b*), anthocyanin accumulation (*Zhang et al., 2015a*), and fatty acid biosynthesis (*Yin et al., 2018*), in tree peony. However, the conclusive studies on the function of genes in tree peony are tough because an efficient genetic transformation system is still not established. Besides, the transgenic technology is time-consuming and laborious for the generation of homozygous lines, especially for plants with long life cycle like tree peony.

Virus-induced gene silencing (VIGS) is an attractively quick strategy for reverse genetic manipulation of non-model plants bypassing the stable transformation process (*Ruiz et al., 1998*; *Burch-Smith et al. 2004*). The VIGS experiment relies on the recombinant virus vector carrying an inserted partial sequence of a target plant gene to initiate RNA-mediated post-transcriptional gene silencing (PTGS), leading to transcript suppression of corresponding homologous gene (*Baulcombe, 1999*; *Burch-Smith et al., 2004*; *Dinesh-Kumar et al., 2011*). In this mechanism, double-stranded chimeric intermediates are first formed during viral replication in plant. Theses foreign intermediate are recognized and cleaved into 21-23 nucleotides of short interfering RNAs (siRNAs) by the enzyme DICER. Next, siRNAs are incorporated into the RNA-induced silencing complex (RISC) and target the complementary transcripts for cleavage, thus resulting in a specific degradation of host mRNA (*Bartel, 2004*; *Senthil-Kumar & Mysore, 2011*). In contrast to gene silencing methods with inverted repeat sequences, VIGS has several advantages as simple plasmid assembly, short implementation cycle, and available identification of embryo-lethal genes (*Reid et al., 2009*).

Many viral vectors have been developed for VIGS assay, including *Apple latent spherical virus* (ALSV), *Barely stripe mosaic virus* (BSMV) (*Holzberg et al., 2002*), *Cucumber mosaic virus* (CMV) (*Tasaki et al., 2016*), *Potato virus X* (PVX) (*Faivrerampant et al., 2004*), *Tobacco mosaic virus* (TMV) (*Kumagai et al., 1995*), and *Tobacco rattle virus* (TRV) (*Ratcliff et al., 2001*). Compared to other viruses, TRV is capable of reaching apical meristem, inducing mild symptoms, and infecting wide range of plant species. Consequently, TRV vector has been widely used for silencing genes in a number of eudicots and monocots (*Purkayastha & Dasgupta, 2009*), such as Arabidopsis (*Burchsmith et al., 2006*), tobacco (*Liu et al., 2002*), tomato (*Quadrana et al., 2011*), petunia (*Sun et al., 2017*), strawberry (*Jia et al., 2011*), rose (*Wu et al., 2016*), gladiolus (*Singh et al., 2013*), wheat, and maize (*Zhang et al., 2017*). At present, the VIGS technique is mostly applied to small herbaceous plants, and only a minority of woody plants achieves the set-up of VIGS system, like physic nut (*Ye et al., 2009*), grape (*Kurth et al., 2012*), and apple (*Yamagishi & Yoshikawa, 2013*). The previous evidences indicate that TRV is one of the most widespread viruses of herbaceous (*P. lactiflora*) and tree (*P. suffruticosa*) peonies (*Garfinkel et al., 2017*). However, whether TRV-based VIGS can be applied to tree peony remains largely unknown.

Reporter gene is an essential component for indicating sites of silencing in VIGS system. PHYTOENE DESATURASE (PDS) is a key enzyme in the biosynthesis of protective carotene (*Cunningham & Gantt, 1998*). Silencing of *PDS* results in characteristic photobleaching symptoms in infected plants (*Stilio et al., 2010*), and therefore it usually serves as a clear reporter. A modified TRV-GFP vector, bearing the coding region of enhanced green fluorescence protein

(EGFP), also provides a visual tool for monitoring virus spread and silencing efficiency. This vector has been successfully tested in several plants, including Arabidopsis, tobacco, rose, strawberry, and chrysanthemum (*Ji et al., 2014*). In this study, we established an effective VIGS system in *P. ostii* triennial seedlings by vacuum infiltration of TRV-*PoPDS* and TRV-GFP. The upper systemically-infected leaves with TRV-*PoPDS* displayed a prominent photobleaching phenotype and decreased *PoPDS* transcripts. GFP fluorescence was observed in TRV-GFP-infiltrated leaves and roots under UV light irradiation. The data we have obtained demonstrated the value of TRV-based VIGS for unraveling the functional significance of genes in tree peony.

Materials and Methods

Plant materials and growth conditions

Three-year-old seedlings of tree peony (*P. ostii* 'Feng Dan') at four weeks post germination were used for VIGS assay (Fig. 1). The whole plant and leaves were agro-infiltrated with disposable syringe and vacuum pressure for infection of TRV constructs, respectively. After inoculation, the tree peony seedlings were rinsed with distilled water once and planted into plastic pots containing a mixture of peat moss and vermiculite in a 3:1 volume ratio. Those plants were first kept in the dark room at 15^{o}C for one week, and then transferred into a growth chamber with a 16 h light/ 8 h dark photoperiod, and a day/night temperature range of 20/18^{o}C. The inoculated and uppermost systemically-infected leaves were used for phenotype observation, expression profile analysis, and GFP fluorescence detection.

126 **Isolation and sequence analysis of *PoPDS***

127 Total RNA was extracted from the *P. ostii* 'Feng Dan' leaves with the TIANGEN RNA Prep
128 Pure Plat kit according to the manufacturer's recommendations (Tiangen, China). The first strand
129 of cDNA was synthesized using PrimeScript® RT reagent Kit with gDNA Eraser (Takara, Japan).
130 Primers were designed to amplify the *PoPDS* coding sequence based on transcriptome data
131 during leaf development of *P. suffruticosa* Andrews (*Luo et al., 2017*). PCR was conducted using
132 Taq DNA polymerase (Invitrogen, USA). The PCR reaction procedure was as follows: a cycle of
133 94 °C for 5min; 35 cycles of 94 °C, 30s, 54 °C, 30s, 72 °C, 30s; a final cycle of 72 °C for 10min.
134 Next, the PCR products were cloned into the pUCm-T vector (TaKaRa, Japan). Positive clones
135 were confirmed by DNA sequencing. Corresponding amino acids were deduced through the
136 ExPASy translate tool (http://web.expasy.org/translate/). Multiple sequence alignment of PoPDS
137 with other similar proteins was performed by CLUSTALW
138 (http://www.genome.jp/tools/clustalw/).
139
140 **Plasmid construction**
141 The TRV1, TRV2, and TRV2-GFP plasmids were kindly provided by Dr. Yule Liu (Tsinghua
142 University, China). To generate the TRV-*PoPDS* construct, a 195-bp *PoPDS* fragment was PCR-
143 amplified using specific primers (Table 1), and cloned into the pUCm-T vector by T4 DNA
144 ligase (Sangon, China). This recombinant plasmid was digested with *Bam*HI and *Eco*RI
145 restriction enzymes, and the *PoPDS* fragment was ligated into corresponding sites of TRV2
146 vector (Fig. 2). The resulting construct was then transformed into *Eacherichia coli* strain DH5α

147 competent cells, which were selected on LB plates containing 50 mg l^{-1} of kanamycin. PCR was
148 used to examine the presence of *PoPDS* insert in the generated construct.
149
150 **Agro-inoculation of TRV vector**
151 TRV1, TRV2, and its derivatives were introduced into *Agrobacterium tumefaciens* strain
152 GV3101 via freeze-thaw method (*Yan et al., 2012*). The transformed bacteria bearing TRV
153 constructs were cultured in LB medium supplemented with 40 mg l^{-1} kanamycin, 20 mg l^{-1}
154 gentamicin, 10 mM MES, and 20 μM acetosyringone at 28 ^{o}C in a growth chamber for 48h.
155 *Agrobacterium* cultures were centrifuged at 4000 *g* for 20 min, and resuspended in the
156 infiltration buffer (10 mM $MgCl_2$, 10mM MES, and 200μM acetosyringone) to a final OD600 of
157 1.0. The cultures containing TRV1 and TRV2 constructs was shaken gently for 4-6 h at room
158 temperature and mixed together in a 1:1 ratio before inoculation. For syringe infiltration, the
159 abaxial sides of two or three fully expanded leaves were injected using a 1-ml needleless syringe.
160 For vacuum infiltration, the whole plants were submerged in the infiltration buffer and subjected
161 to 0.1 MPa vacuum pressure for 20 min. Approximately 50 tree peony seedlings were inoculated
162 by vacuum method.
163
164 **Semi-quantitative RT-PCR and quantitative real-time PCR**
165 The total RNA was extracted from inoculated and systemically-infected leaves of tree peony
166 seedlings, and purified with RNase-free DNase (Takara, Japan). First-strand cDNA as the
167 template for PCR was synthesized from 2-5μg of total RNA. Three primer pairs were designed to

168 detect the presence of TRV (Table 1). Since the forward and reverse primers of TRV2-2 covered
169 the multiple cloning sites (MCS), the size of resulting product varied depending on the inserts in
170 the site, whereas the TRV1 and TRV2-1 primers led to the bands with the same sizes (*Sun et al.,*
171 *2016*). The PCR products were analyzed through electrophoresis using a Molecular Imager Gel
172 Doc XR+ System (Bio-Rad, USA). Quantitative real-time PCR (qRT-PCR) was carried out
173 using SYBR Premix Ex Taq II (Takara, Japan) in a 20-μl PCR mixture and analyzed by a
174 StepOnePlus Real-time PCR System (Applied Biosystems, USA). 18S-26S internal transcribed
175 spacer was used as an internal control to normalize the expression data (*Zhang et al., 2018*). The
176 PCR primers, used for the determination of transcript abundances of *PoPDS*, were designed
177 outside the region of the inserted fragment to avoid amplification of the fragment included in
178 TRV2 construct.
179
180 **GFP imaging**
181 Transient assay of GFP in in the inoculated leaf cells of *P. ostii* was conducted based on the
182 agro-infiltration with TRV-GFP. GFP fluorescence was detected and photographed using a laser
183 scanning confocal microscope (Leica TCS SP8).
184
185 **Western blot**
186 A GFP-specific antibody (Abcam Inc) was used to implement western blot analysis. Proteins
187 were extracted from leaves and roots of *P. ostii* plants infected with TRV-GFP, with 300 μL
188 extraction buffer (100 mM Tris pH=6.8, 2.5 % SDS, 100 mM dithiothreitol, 100 mM NaCl, and

189 10% glycerol). Bradford assay was used to determine protein quantities, and equal amounts of
190 proteins for each sample were separated by 10% SDS-PAGE (*Bradford, 1976*). Next, proteins
191 were transferred to a polyvinylidene difluoride membrane (GE healthcare). CP-GFP was
192 detected after an overnight incubation at room temperature with a 1:10,000 dilution of the anti-
193 GFP antibody conjugated to alkaline phosphatase (*Bedoya et al., 2012*). Alkaline phosphatase
194 was detected using a chemiluminescent substrate (CSPD; Roche) and exposed to X-ray film
195 (Kodak X-OMAT BT Film/XBT-1).
196
197 **Results**
198 **Comparison of the agro-infiltration methods**
199 In view of the woody characteristics of tree peony, choosing a plant with optimal age and size for
200 VIGS assay is pre-requisite. Three-year-old young plantlets were therefore used because of their
201 delicate underground roots, small plant type, and high occurrence of new leaves (Fig. 1a). To
202 determine the most appropriate method of *Agrobacterium*-mediated TRV infection in tree peony,
203 leaf syringe-infiltration and seedling vacuum-infiltration were selected for comparison (Fig. 1b).
204 These two methods acted on the leaf back and whole plant, respectively. We found that the
205 vacuum way brought about a more sufficient permeation of bacterial cultures through the abaxial
206 leaf surface than the syringe way, which made the infiltration happen only at the inoculation sites.
207 The syringe infiltration inevitably caused obvious mechanical damage to leaf tissues (Fig. 1c).
208 Semi-quantitative RT-PCR analysis indicated that TRV1 and TRV2 transcripts were detected in
209 all inoculated leaves by both infiltration methods, and not in untreated leaves (Fig. 1d).

210 According to the results, vacuum infiltration was used for subsequent gene-silencing experiments.

211

212 **Identification of *PoPDS***

213 Using the transcriptome data obtained from developing leaves of tree peony, we PCR-amplified
214 the open reading frame (ORF) nucleotide sequence of *phytoene desaturase* (*PDS*) of *P. ostii*,
215 annotated as *PoPDS*, which was commonly used as a reporter for silencing. *PoPDS* encodes a
216 protein of 575 amino acids, and conserved domain analysis revealed a putative dinucleotide
217 binding domain in its deduced protein sequence. Multiple sequence alignments showed that
218 PoPDS amino acids shared high similarity with the homologies from other plant species, such as
219 *Vitis vinifera*, *Nicotiana tabacum*, *Arabidopsis thaliana*, and *Petunia hybrida* (Fig. 2). The full-
220 length peptides of PoPDS had 83.3%, 82.09%, 79.96%, and 80.7% identities with those of four
221 plant species, respectively.

222

223 **Silencing of *PoPDS* in *P. ostii* leaves**

224 To assess the feasibility of TRV-based VIGS in tree peony, we introduced a 195-bp conserved
225 fragment of *PoPDS* into TRV2 vector, and generated a TRV-*PoPDS* recombinant (Fig. 3). Upon
226 *Agrobacterium*-mediated infection, similar necrotic symptoms occurred in the edge of leaves
227 infiltrated with TRV empty vector and TRV-*PoPDS*, while the remaining area seemed normal
228 (Fig. 4a). Approximately 52% of seedlings exhibited a remarkable photobleaching phenotype in
229 the first newly developed leaves at 4 weeks post inoculation. White spots or sectors were clearly
230 observed throughout the upper leaves particularly around leaf main veins. This phenotype

231 remained stable and persisted for about 5 months under growth chamber conditions. It indicated
232 that the *PoPDS* of tree peony could be silenced by VIGS and TRV infection was systemically
233 established.

234 To confirm the correlation of leaf photobleaching with the presence of the viral vectors, TRV
235 accumulation was examined using semi-quantitative RT-PCR. DNA fragments of TRV1 and
236 TRV2 were detected in TRV empty vector- and TRV-*PoPDS*-infected leaves, but not in the
237 mock control plants (Fig. 4b). When using primers covering MCS of TRV2 vector, a fragment
238 carrying *PoPDS* insert was detected in the leaves agro-infiltrated with TRV-*PoPDS*. 18S-26S
239 internal transcribed spacer was referred as an internal control for normalization of gene
240 expression. QRT-PCR analysis demonstrated that transcript abundances of *PoPDS* were
241 significantly reduced in photobleached leaves of plants infiltrated with TRV-*PoPDS*, compared
242 with that in mock- and TRV empty vector-inoculated seedlings (Fig. 4c). These results suggested
243 that the leaf photobleaching phenotype was definitely initiated by *PoPDS* silencing.

244

245 **Validation of TRV-GFP in *P. ostii* leaves and roots**

246 Apart from TRV-*PoPDS*, another visualizable vector TRV-GFP, in which the EGFP coding
247 sequence was fused to coat protein ORF of TRV2, was used for infiltration to monitor virus
248 spread in *P. ostii*. Under a confocal microscope, GFP fluorescence was observed in the newly
249 emerging leaves and roots of plants at 5 days post inoculation with TRV-GFP, indicating the
250 capability of TRV vector to express foreign genes in different tree peony tissues. No
251 fluorescence signals were detected in mock control leaves and roots (Fig. 5).

252 Moreover, we performed western blot analysis to check the expression of GFP protein in
253 infected leaves and roots. As illustrated in Fig. 6a, GFP proteins were accumulated in the leaves
254 and roots of plants inoculated with TRV-GFP, whereas no GFP bands were found in control
255 plants. By contrast, the GFP abundances in infected roots appeared to be much higher than that
256 in infected leaves (Fig. 6a). Semi-quantitative RT-PCR analysis revealed a consistent variance
257 that the roots exhibited more transcripts of TRV1, TRV2, and GFP than the leaves (Fig. 6b). The
258 data suggested that the systemic movement of TRV vector in tree peony plants could be
259 effectively supervised via the GFP-tagged expression.
260

261 **Discussion**

262 Besides the significance of floral characteristics, tree peony roots containing some special
263 secondary metabolites are generally used as traditional Chinese medical materials, and its leaves
264 has excellent ornamental values owing to its changeable color during the early growth period
265 (*Luo et al., 2017*; *Li et al., 2018*). Therefore, there are considerable interests in evaluating the
266 gene function in both roots and leaves of tree peony. However, an effective genetic
267 transformation system is still unavailable in tree peony because of severe callus browning and
268 tough plant regeneration (*Liu & Jia, 2010*). Few studies on molecular functional identification
269 have been performed in tree peony due to this limitation. It seems likely that a transient
270 expression system for up- or -down-regulation of genes in tree peony would be greatly needed.
271 VIGS technique has been widely used in various plant species as a rapid, convenient, and
272 efficient tool for functional assessment of genes (*Wege et al., 2007*; *Velásquez et al., 2009*). In

the present study, whether TRV-based vector could be used for silencing endogenous genes in tree peony was investigated. Our results demonstrated that the conventional leaf syringe-infiltration method is laborious and it resulted in an inadequate infiltration to *P. ostii* leaves, when compared with seeding vacuum-infiltration. It is quite likely that the physiological structure of tree peony leaf affected the entering of agrobacterial mixture. Not many stomatal apparatus existed in the lower epidermis of tree peony young leaf, and its leaf mesophyll cells were divided into a large number of vein islets by reticulate vein networks. Only a small-scale of leaf could be effectively infected with TRV constructs via syringe injection. Additionally, the thin tree peony leaves were prone to suffer mechanical damage from syringe-infiltration method. Previous studies also showed that the vacuum approach was more effective than other infiltration methods in woody plants (*Ye et al., 2009*; *Liu et al., 2014*). Thus, a vacuum-infiltration into the whole plant is probably considered as a good choice, when it comes to species that are difficult to infect.

Concerning the experimental materials for inoculation, it is well known that tree peony has a long juvenile stage that commonly lasts for about 3 years, during which the root is the main growing part (*Wang et al., 2015*). This development feature confined the application of VIGS on tree peony plants. Three-year-old seedlings of tree peony were consequently selected as agro-inoculated objects in our work. Since the plants at this stage were favorable to vacuum infiltration in size, and on the other hand to sprouting of upper new leaves. A visual silencing phenotype of marker gene, such as *PDS*-silenced leaf photobleaching or *chalcone synthase* (*CHS*)-silenced white-corollas phenotypes, requires upspring of systemically-infected tissues. Our

294 results proved that a significant gene silencing took place in newly-developed leaves of triennial
295 *P. ostii* plants. Because the reproductive buds of triennial tree peony plants didn't take shape, a
296 trial of gene silencing in tree peony floral organs via VIGS will be made in the following work.

297 *PDS* has been frequently used as an indicator gene in VIGS systems because the silencing of
298 *PDS* reduces photoprotective carotenoid levels in green tissues and thereby leads to chlorophyll
299 photooxidation and tissue bleaching (*Kumagai et al., 1995*). In this study, we cloned the *PDS*
300 gene from *P. ostii* leaves and constructed the TRV-*PoPDS* vector to unravel the function of
301 *PoPDS* and verify the possibility of VIGS in tree peony. After infiltration with TRV-*PoPDS*, an
302 expected silencing phynotype (photobleaching) was observed in systemically-infected leaves,
303 while the directly inoculated leaves didn't except some lesions resembling TRV empty vector-
304 treated leaves. The results mentioned above indicated that a systemic TRV viral infection was
305 established, and it was essential for the VIGS application. The silencing of *PoPDS* also
306 demonstrated that TRV-based VIGS could be used as an effective method towards functional
307 characterization of genes in tree peony plants.

308 It is noteworthy that almost all photobleached leaves resulting from TRV-*PoPDS* infection
309 exhibited variegated phenotypes as white spots or sectors not completely white (Fig. 4a), and we
310 hypothesized that multiple factors may contribute to it. The post-inoculation growth temperature
311 largely influences the efficiency of VIGS-based gene silencing. It has been reported that low
312 temperature enhances gene silencing efficiency when TRV-mediated VIGS is employed in
313 tomato (*Fu et al., 2006*). But a conflicting finding is that low temperature suppresses gene
314 silencing through the prevention of siRNA formation in *N. benthamiana* (*Szittya et al., 2003*).

315 The length of inserted fragment in viral vector is also closely associated with gene silencing
316 efficiency. As reported previously, different lengths of *PDS* inserts result in varied
317 photobleaching patterns and ranges in TRV-infected tobacco (*Liu & Page, 2008*; *Ye et al., 2009*).
318 Our VIGS procedure hence requires further optimization in temperature and inserted fragment
319 size in future work. Furthermore, the *PoPDS*-silenced phenotypes were particularly significant
320 along the leaf vein (Fig. 4a). It is in agreement with the results that viral propagation and the
321 silenced systemic response occur mainly along the vascular bundle system (*Wege et al., 2007*).

322 In order to visualize viral accumulation in infiltrated tree peony plants, the TRV-GFP vector
323 was used. The GFP, a fluorescent protein from jellyfish (*Aequorea victoria*), does not participate
324 in biological processes of plants. Its gene was overexpressed driven by the 35S promoter by TRV
325 vector and used as a traceable marker to indicate the presence of virus (*Quadrana et al., 2011*).
326 In present work, green fluorescence was observed in the roots and leaves of infected tree peony
327 seedlings at 5 dpi, and the abundances of TRV1, TRV2, and GFP were also detected (Fig. 5).
328 The concentration of GFP protein was able to reflect the viral load and degree of silencing (*Ji et*
329 *al., 2014*). We found a higher transcript and protein levels of GFP in roots than that in leaves. It
330 is concluded that virus infection may happen mainly in roots at first and then spread into newly-
331 developed leaves after vacuum infiltration. Previous findings proved that TRV virus possesses
332 the ability to move efficiently within the roots of infected plants (*Macfarlane & Popovich, 2000*).
333 Future work will examine the underlying mechanism discrepancy of TRV replication and
334 movement in roots and leaves of tree peony. Altogether, it suggested that the TRV-GFP vector
335 was positive to tree peony plants and suitable for monitoring the systemic spread of TRV

carrying target gene fragments. An advantage is that the employment of TRV-GFP construct could avoid the destruction of the photosynthetic apparatus caused by *PDS*-silenced leaf photobleaching.

Conclusion

In conclusion, our results indicated that an effective TRV-based VIGS system was established in *P. ostii* based on TRV-*PoPDS* and TRV-GFP constructs. Seedling vacuum-infiltration was determined as an appropriate method for *Agrobacterium*-mediated infection of TRV, compared with leaf syringe-infiltration. A remarkable photobleaching phenotype was observed in TRV-*PoPDS*-infected upper new leaves, which was concomitant with substantial reduction in *PoPDS* transcripts. The detection of GFP fluorescence and accumulation levels in leaves and roots infected with TRV-GFP revealed a valid means to monitor the viral spread in different tissues of tree peony plants. Thus, this system we developed will be greatly helpful to characterize the function of genes associated with various molecular and physiological processes in tree peony.

Acknowledgements

We thank Xiang Li and Xiaotong Ji for experimental assistance in agro-infiltration with syringe and vacuum. We are grateful to Yule Liu's favor for kindly providing TRV-GFP vector.

ADDITIONAL INFORMATION AND DECLARATIONS

Funding

This work was supported by the National Forestry Public Welfare Research Project of China (Project No. 201404701), National Science Foundation of China (Project No. 31800599), and China Postdoctoral Science Foundation (Project No. 2018M631211).

Competing Interests

The authors declare there are no competing interests.

Author Contributions

Yanlog Zhang, Lixin Niu, and Daoyang Sun conceived and designed the research.

Lihang Xie, Qingyu Zhang, Jiayuan Hu and Weizong Yang conducted the experiments.

Lihang Xie and Qingyu Zhang organized the data and wrote the manuscript.

Daoyang Sun and Yanlong Zhang commented and revised the manuscript.

All authors read and approved the final manuscript.

References

Bartel DP. 2004. MicroRNAs: genomics, biogenesis, mechanism, and function. *Cell* **116:**281–297

Baulcombe D. 1999. Viruses and gene silencing in plants. *Arch Virol Suppl* **15:**189–201

Bedoya LC, Martínez F, Orzáez D, Daròs JA. 2012. Visual tracking of plant virus infection and movement using a reporter MYB transcription factor that activates anthocyanin biosynthesis. *Plant Physiology* **158:**1130–1138

Bradford M. 1976. A rapid and sensitive method for quantitation of microgram quantities of protein utilizing the principle of proteindye binding. *Analytical Biochemistry* **72:**248–254

Burch-Smith T, Anderson J, Martin GK, Sp. 2004. Applications and advantages of virus-induced gene silencing for gene function studies in plants. *Plant Journal* **39:**734–746

Burchsmith TM, Schiff M, Liu Y, Dineshkumar SP. 2006. Efficient virus-induced gene silencing in Arabidopsis. *Plant Physiology* **142:**21–27

Cheng F, Li J, and Yu L. 1998. Exportation of Chinese Tree Peonies (Mudan) and their developments in other countries.II.Wild species. *Estuarine Coastal & Shelf Science* **73:**223–235.

Cunningham FX, and Gantt E. 1998. GENES AND ENZYMES OF CAROTENOID BIOSYNTHESIS IN PLANTS. *Annual Review of Plant Biology* **49:**557-583.

Dinesh-Kumar SP, Anandalakshmi R, Marathe R, Schiff M, and Liu Y. 2011. Virus-induced gene silencing. *Methods Mol Biol* **236:**287-294.

Faivrerampant O, Gilroy EM, Hrubikova K, Hein I, Millam S, Loake GJ, Birch PRJ, Taylor MA, and Lacomme C. 2004. Potato Virus X-Induced Gene Silencing in Leaves and Tubers of Potato. *Plant Physiology* **134:**1308-1316.

Fu DQ, Zhu BZ, Zhu HL, Zhang HX, Xie YH, Jiang WB, Zhao XD, and Luo KB. 2006. Enhancement of virus-induced gene silencing in tomato by low temperature and low humidity. *Molecules & Cells* **21:**153-160.

Garfinkel AR, Lorenzini M, Zapparoli G, and Chastagner G. 2017. Botrytis euroamericana, a new species from peony and grape in North America and Europe. *Mycologia* **109:**495-507.

Holzberg S, Brosio P, Gross CS, and Pogue GP. 2002. Barley stripe mosaic virus‐induced gene silencing in a monocot plant. *Plant Journal* **30:**315-327.

Ji T, Pei H, Shuai Z, Chen J, Wen C, Yang R, Meng Y, Jie Y, Gao J, and Nan M. 2014. TRV–GFP: a modified Tobacco rattle virus vector for efficient and visualizable analysis of gene function. *Journal of Experimental Botany* **65:**311-322.

Jia HF, Chai YM, Li CL, Lu D, Luo JJ, Qin L, and Shen YY. 2011. Abscisic acid plays an important role in the regulation of strawberry fruit ripening. *Plant Physiology* **157:**188.

Kumagai MH, Donson J, Dellacioppa GR, Harvey D, Hanley KM, and Grill LK. 1995. Cytoplasmic inhibition of carotenoid biosynthesis with virus-derived RNA. *Proceedings of the National Academy of Sciences of the United States of America* **92:**1679-1683.

Kurth EG, Peremyslov VV, Prokhnevsky AI, Kasschau KD, Miller M, Carrington JC, and Dolja VV. 2012. Virus-Derived Gene Expression and RNA Interference Vector for Grapevine. *Journal of Virology* **86:**6002-6009.

Li C, Hui DU, and Wang L. 2009. Flavonoid Composition and Antioxidant Activity of Tree Peony (Paeonia Section Moutan) Yellow Flowers. *Journal of Agricultural & Food Chemistry* **57:**8496-8503.

Li J, Han J, Hu Y, and Yang J. 2016. Selection of Reference Genes for Quantitative Real-Time PCR during Flower Development in Tree Peony (*Paeonia suffruticosa Andr.*). *Front Plant Sci* **7:**516.

Li S, Wu Q, Yin D, Feng C, Liu Z, and Wang L. 2018. Phytochemical variation among the traditional Chinese medicine Mu Dan Pi from Paeonia suffruticosa (tree peony). *Phytochemistry* **146:**16-24.

Liu E, and Page JE. 2008. Optimized cDNA libraries for virus-induced gene silencing (VIGS) using tobacco rattle virus. *Plant Methods* **4:**5-5.

Liu HC, and Jia WQ. 2010. Establishment of plantlet regeneration system of tree peony through lateral buds cutting and carving. *Acta Horticulturae Sinica* **37:**1471-1476.

Liu Y, Schiff M, and Dineshkumar SP. 2002. Virus‐induced gene silencing in tomato. *Plant Journal* **31:**777-786.

Liu Y, Wei S, Zeng S, Huang W, Di L, Hu W, Shen X, and Ying W. 2014. Virus-induced gene silencing in two novel functional plants, Lycium barbarum L. and Lycium ruthenicum Murr. *Scientia Horticulturae* **170:**267-274.

Luo J, Shi Q, Niu L, and Zhang Y. 2017. Transcriptomic Analysis of Leaf in Tree Peony Reveals Differentially Expressed Pigments Genes. *Molecules* **22:**324.

Macfarlane SA, and Popovich AH. 2000. Efficient expression of foreign proteins in roots from tobravirus vectors. *Virology* **267:**29-35.

Purkayastha A, and Dasgupta I. 2009. Virus-induced gene silencing: a versatile tool for discovery of gene functions in plants. *Plant Physiology and Biochemistry* **47:**967-976.

Quadrana L, Rodriguez MC, Lopez MG, Bermudez L, Nunesnesi A, Fernie AR, Descalzo A, Asis R, Rossi MM, and Asurmendi S. 2011. Coupling Virus-Induced Gene Silencing to Exogenous Green Fluorescence Protein Expression Provides a Highly Efficient System for Functional Genomics in Arabidopsis and across All Stages of Tomato Fruit Development. *Plant Physiology* **156:**1278-1291.

Ratcliff F, ., Martin-Hernandez AM, and Baulcombe DC. 2001. Technical Advance. Tobacco rattle virus as a vector for analysis of gene function by silencing. *Plant Journal* **25:**237–245.

Reid M, Chen JC, and Jiang CZ. 2009. Virus-Induced Gene Silencing for Functional Characterization of Genes in Petunia.

Ruiz MT, Voinnet O, and Baulcombe DC. 1998. Initiation and Maintenance of Virus-Induced Gene Silencing. *The Plant Cell* **10:**937-946.

Senthilkumar M, and Mysore KS. 2011. New dimensions for VIGS in plant functional genomics. *Trends in Plant Science* **16:**656-665.

Singh A, Kumar P, Jiang CZ, and Reid MS. 2013. TRV Based Virus Induced Gene Silencing in Gladiolus (Gladiolus grandiflorus L.), A Monocotyledonous Ornamental Plant. *International Journal of Plant Research* **26:**170.

Stilio VS, Di, Kumar RA, Oddone AM, Tolkin TR, Patricia S, and Kacie MC. 2010. Virus-induced gene silencing as a tool for comparative functional studies in Thalictrum. *Plos One* 5:e12064.

Sun D, Li S, Niu L, Reid MS, Zhang Y, and Jiang C. 2017. PhOBF1, a petunia ocs element binding factor, plays an important role in antiviral RNA silencing. *Journal of Experimental Botany* **68:**915-930.

Sun D, Nandety RS, Zhang Y, Reid MS, Niu L, and Jiang C. 2016. A petunia ethylene-responsive element binding factor, PhERF2, plays an important role in antiviral RNA silencing. *Journal of Experimental Botany* **67:**3353-3365.

Szittya G, Silhavy D, Molnar A, Havelda Z, Lovas A, Lakatos L, Banfalvi Z, and Burgyan J. 2003. Low temperature inhibits RNA silencing-mediated defence by the control of siRNA generation. *The EMBO Journal* **22:**633-640.

Tasaki K, Terada H, Masuta C, and Yamagishi M. 2016. Virus-induced gene silencing (VIGS) in Lilium leichtlinii using the Cucumber mosaic virus vector. *Plant Biotechnology* **33:**373-381.

Tian J, Pei H, Zhang S, Chen J, Chen W, Yang R, Meng Y, You J, Gao J, and Ma N. 2014. TRV–GFP: a modified Tobacco rattle virus vector for efficient and visualizable analysis of gene function. *Journal of Experimental Botany* **65:**311-322.

Velásquez AC, Chakravarthy S, and Martin GB. 2009. Virus-induced gene silencing (VIGS) in Nicotiana benthamiana and tomato. *Journal of Visualized Experiments* **28:**: 1292.

Wang S, Beruto M, Xue J, Zhu F, Liu C, Yan Y, and Zhang X. 2015. Molecular cloning and potential function prediction of homologous SOC1 genes in tree peony. *Plant Cell Reports* **34:**1459-1471.

Wege S, Scholz A, Gleissberg S, and Becker A. 2007. Highly Efficient Virus-induced Gene Silencing (VIGS) in California Poppy (Eschscholzia californica): An Evaluation of VIGS as a Strategy to Obtain Functional Data from Non-model Plants. *Annals of Botany* **100:**641-649.

Wu J, Cai C, Cheng F, Cui H, and Zhou H. 2014. Characterisation and development of EST-SSR markers in tree peony using transcriptome sequences. *Molecular Breeding* **34:**1853-1866.

Wu L, Ma N, Jia Y, Zhang Y, Feng M, Jiang CZ, Ma C, and Gao J. 2016. An ethylene-induced regulatory module delays flower senescence by regulating cytokinin content. *Plant Physiology* **173**:pp.01064.02016.

Yamagishi N, and Yoshikawa N. 2013. Highly Efficient Virus-Induced Gene Silencing in Apple and Soybean by Apple Latent Spherical Virus Vector and Biolistic Inoculation. *Methods of Molecular Biology* **975**:167-181.

Yan H, Fu D, Zhu B, Liu H, Shen X, and Luo Y. 2012. Sprout vacuum-infiltration: a simple and efficient agroinoculation method for virus-induced gene silencing in diverse solanaceous species. *Plant Cell Reports* **31**:1713-1722.

Ye J, Qu J, Bui HTN, and Chua N. 2009. Rapid analysis of Jatropha curcas gene functions by virus‐induced gene silencing. *Plant Biotechnology Journal* **7**:964-976.

Yin DD, Xu WZ, Shu QY, Li SS, Wu Q, Feng CY, Gu ZY, and Wang LS. 2018. Fatty acid desaturase 3 (PsFAD3) from Paeonia suffruticosa reveals high α -linolenic acid accumulation. *Plant Science* **274**:212-222.

Zhang J, Yu D, Zhang Y, Liu K, Xu K, Zhang F, Wang J, Tan G, Nie X, and Ji Q. 2017. Vacuum and Co-cultivation Agroinfiltration of (Germinated) Seeds Results in Tobacco Rattle Virus (TRV) Mediated Whole-Plant Virus-Induced Gene Silencing (VIGS) in Wheat and Maize. *Frontiers in Plant Science* **8**.

Zhang Q, Yu R, Xie L, Rahman M, Kilaru A, Niu L, and Zhang Y. 2018. Fatty Acid and Associated Gene Expression Analyses of Three Tree Peony Species Reveal Key Genes for α-Linolenic Acid Synthesis in Seeds. *Frontiers in Plant Science* **9**.

Zhang Y, Cheng Y, Ya H, Xu S, and Han J. 2015a. Transcriptome sequencing of purple petal spot region in tree peony reveals differentially expressed anthocyanin structural genes. *Frontiers in Plant Science* **6**.

Zhang Y, Zhang L, Gai S, Liu C, and Lu S. 2015b. Cloning and expression analysis of the R2R3-PsMYB1 gene associated with bud dormancy during chilling treatment in the tree peony (Paeonia suffruticosa). *Plant Growth Regulation* **75**:667-676.

Table 1(on next page)

Primers used for RT-PCR amplification and construction of recombinant TRV2 plasmids

Table 1 Primers used for RT-PCR amplification and construction of recombinant TRV2 plasmids.

Primer name	Nucleotide sequence (5'-3')	Purpose	Size
PoPDS-F1	TCGGAGTTGGGTTCGCTGC	Cloning of *PoPDS* coding region	1797bp
PoPDS-R1	ATTCTGATGTGTTTTGTAGCC		
PoPDS-F2	CAGCCGATTTGATTTCCTTG	Cloning of inserted fragment for VIGS	195bp
PoPDS-R2	CCTTGTTTTCTCATCCAGTC		
PoPDS-F3	AGTCATTGGGGGGTCAGGTCCG	RT-PCR	312bp
PoPDS-R3	CAGCATACACACTCAGAAGGGG		
TRV1-F	CAGTCTATACACAGAAACAGA	TRV1-RNA detection	463bp
TRV1-R	GACGTGTGTACTCAAGGGTT		
TRV2-1F	GGCTAACAGTGCTCTTGGTG	TRV2-RNA detection	359bp
TRV2-1R	GTATCGGACCTCCACTCGC		
TRV2-2F	CGAGTGGAGGTCCGATACG	TRV2-RNA (containing inserted fragment) detection	Depending on insert
TRV2-2R	CGGTTCATGGATTCGGTTAG		
GFP-F	ATGGCCAACACTTGTCACTACTT	GFP-RNA detection	260bp
GFP-R	ATTCCAATTTGTGTCCAAGAATG		
18S-26S-ITS-F	ACCGTTGATTCGCACAATTGGTCA	RT-PCR	150bp
18S-26S-ITS-R	TACTGCGGGTCGGCAATCGGACG		

Figure 1

Comparison of syringe-infiltration and vacuum-infiltration methods with the TRV empty vector

a Three-year-old *P. ostii* plantlets at 4 weeks post germination used for agro-infiltration. **b** Schematic depiction of *Agrobacterium*-mediated TRV inoculation in *P. ostii* plants using syringe and vacuum methods. **c** The *P. ostii* leaves subjected to syringe- and vacuum-infiltration with TRV empty vector. **d** Semi-quantitative RT-PCR analysis of TRV1 and TRV2-1 accumulation levels in TRV empty vector-inoculated leaves by syringe and vacuum methods. 18S-26S internal transcribed spacer (18S-26S-ITS) was used as internal standard.

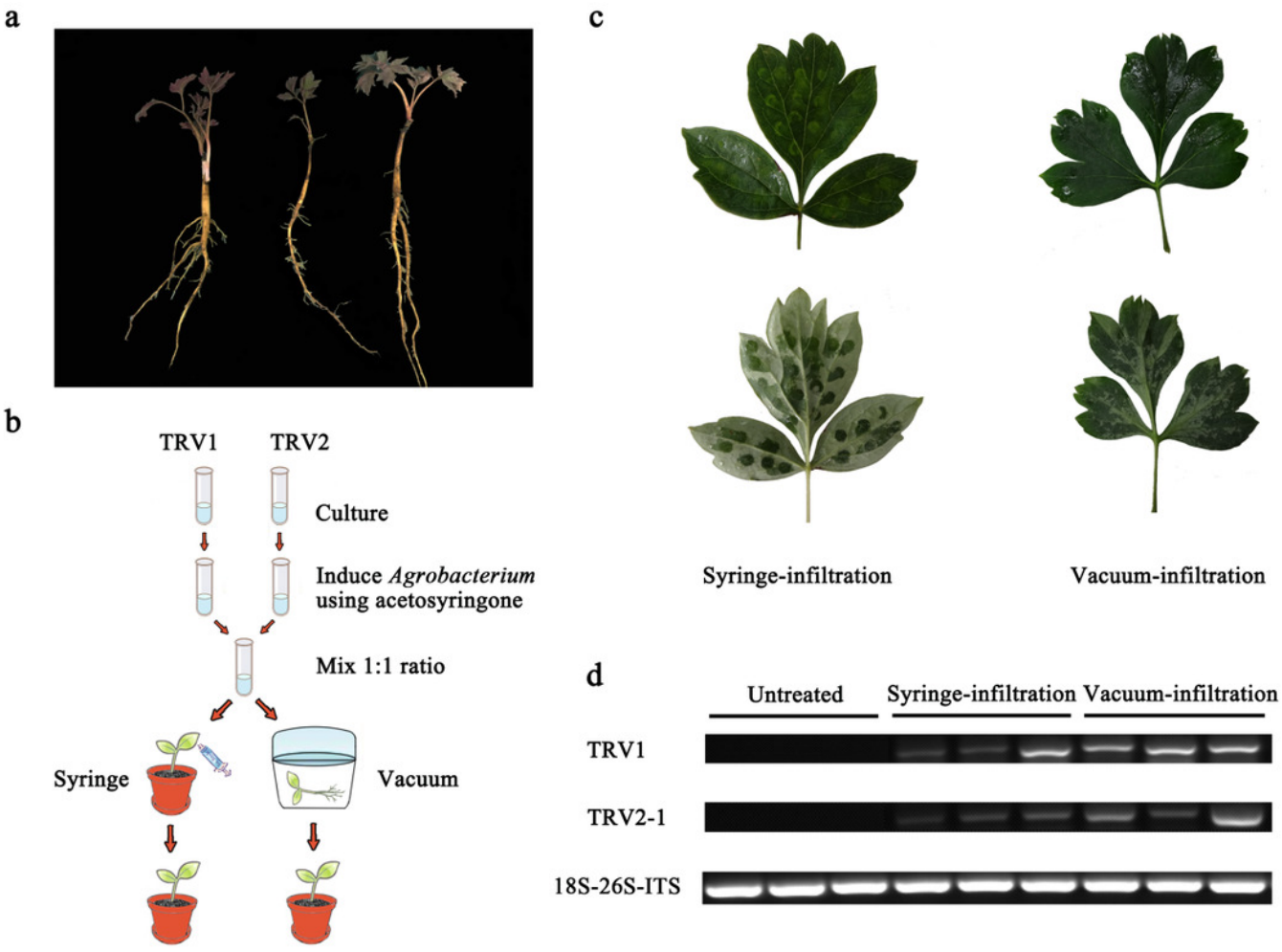

Figure 2

Multiple sequence alignment of deduced amino acids of PoPDS with other homologies, including *Vitis vinifera* VvPDS, *Nicotiana tabacum* NtPDS, *Arabidopsis thaliana* AtPDS, and *Petunia hybrida* PhPDS

Sequences were aligned using ClustalW program. The N-terminus and transient sequence and putative dinucleotide-binding domain are underlined. Red box denotes a conserved region in PDS protein sequences for VIGS. Black background represents identical amino acid residues.

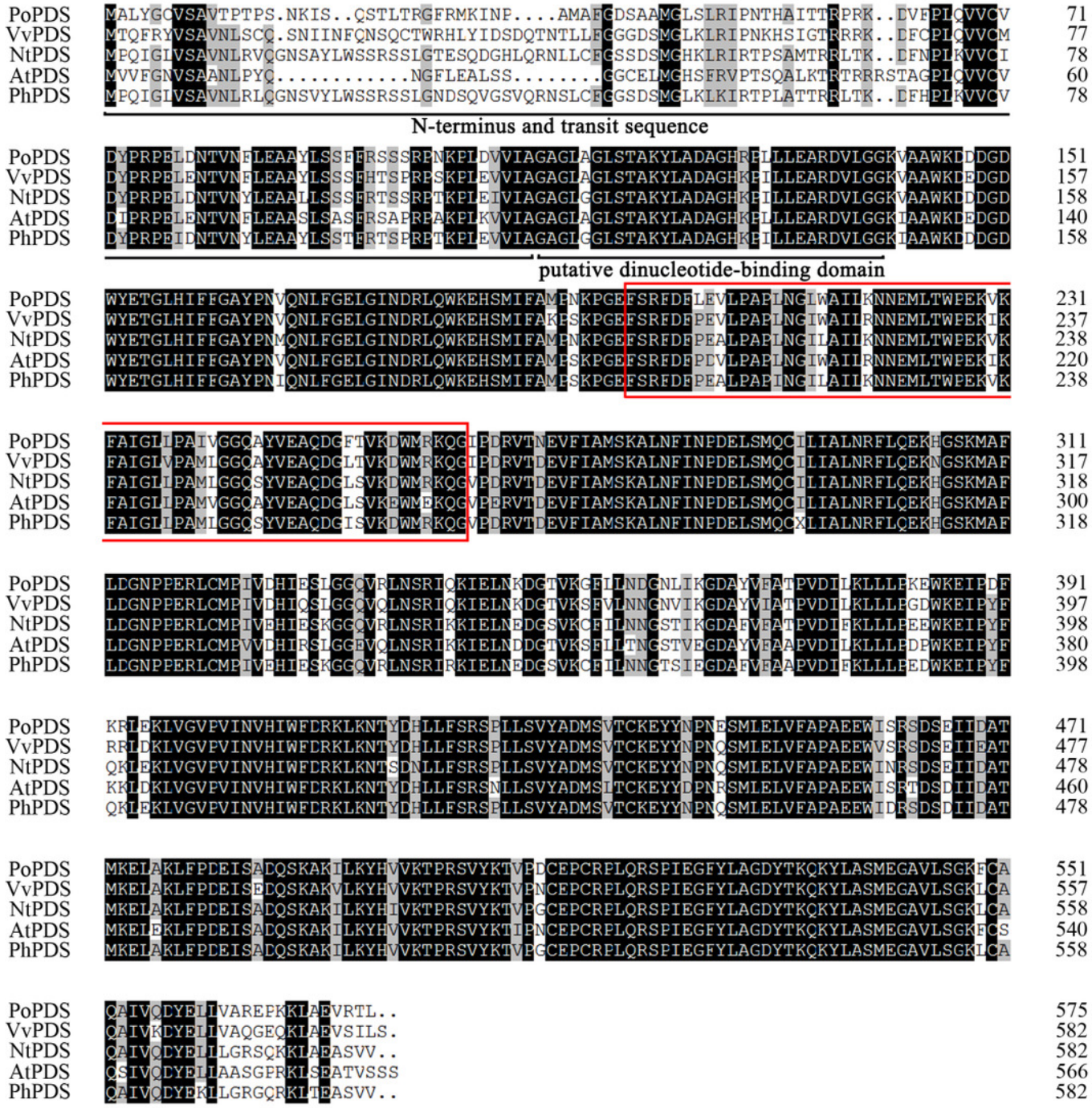
PoPDS
VvPDS
NtPDS
AtPDS
PhPDS
N-terminus and transit sequence
putative dinucleotide-binding domain

Figure 3

Schematic representation of TRV constructs used in this study

a The cDNA of *PoPDS* insert for its introduction into TRV vector. PoPDS-F1/PoPDS-R1 was used to amplify the open reading frame region of *PoPDS*, PoPDS-F2/PoPDS-R2 targeted the inserted fragment of *PoPDS*, and PoPDS-F3/PoPDS-R3 was designed for quantitative real-time PCR. **b** The structures of TRV1, TRV2, TRV2-*PoPDS*, and TRV2-GFP. The arrows indicate the different primer pairs for examining TRV1, TRV2-1, TRV2-2, and GFP transcript levels. LB left border, RB right border, MP movement protein, 16K 16 Kd protein, Rz self-cleaving ribozyme, NOS_t NOS terminator, CP coat protein, MCS multiple cloning site.

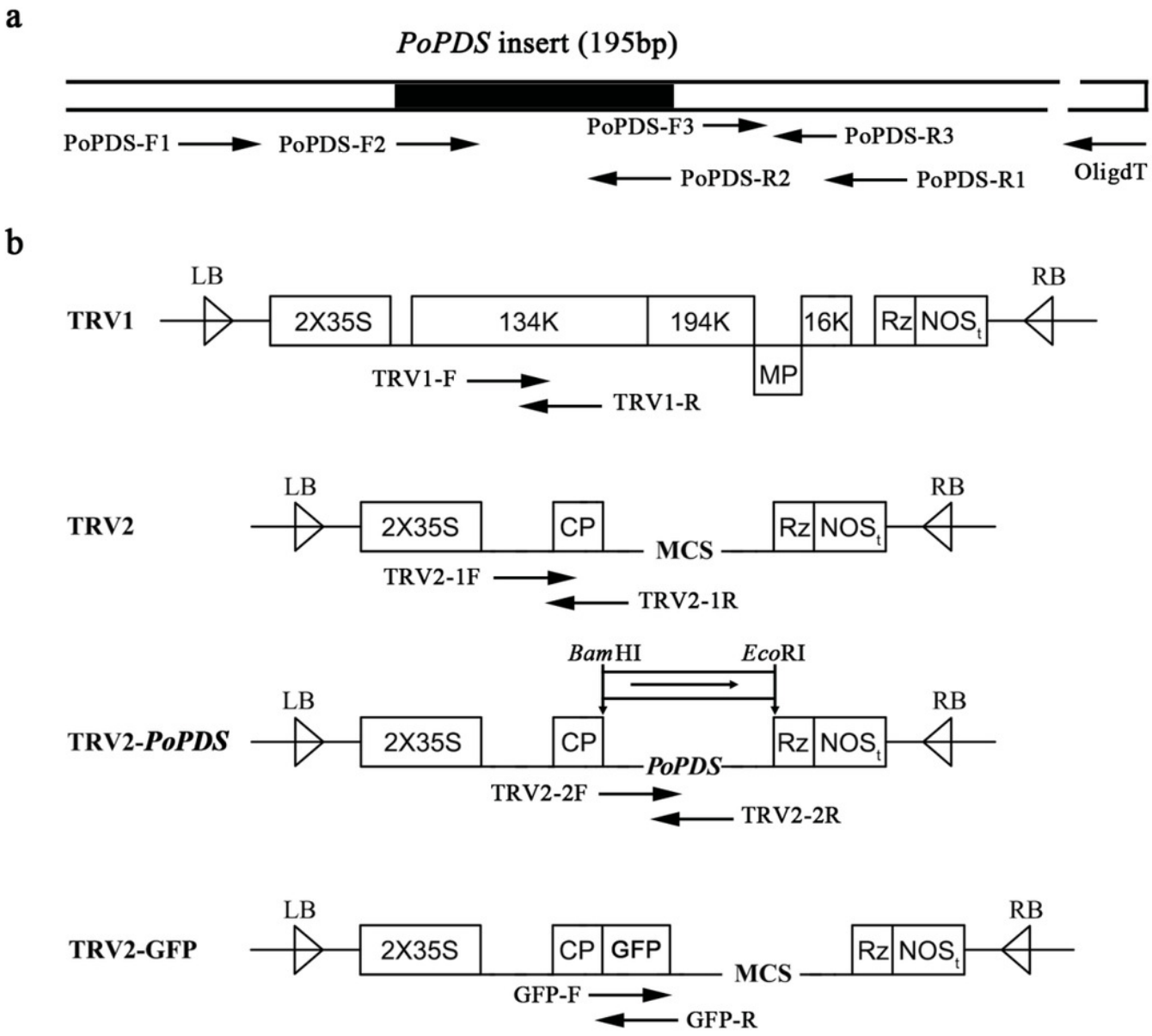
a
PoPDS insert (195bp)
PoPDS-F1
PoPDS-F2
PoPDS-F3
PoPDS-R3
PoPDS-R2
PoPDS-R1
OligdT
b
TRV1
LB
2X35S
134K
194K
16K
MP
Rz
NOS
RB
TRV1-F
TRV1-R
TRV2
CP
MCS
TRV2-1F
TRV2-1R
BamHI
EcoRI
TRV2-PoPDS
PoPDS
TRV2-2F
TRV2-2R
TRV2-GFP
GFP
GFP-F
GFP-R

Figure 4

Silencing of *PoPDS* in *P. ostii* leaves infected with TRV-*PoPDS*

a Representative phenotypes of mock treated, TRV- (empty vector), and TRV-*PoPDS*-infected leaves in *P. ostii* seedlings. Photobleaching phenotypes were observed in the first newly-developed leaves of seedlings at 5 weeks post infiltration with TRV-*PoPDS*. **b** Semi-quantitative RT-PCR analysis of TRV1 and TRV2 accumulation levels in systemically-infected *P. ostii* leaves. TRV2-1 targets the region upstream of MCS and produced the same sizes of products, while the primers for TRV2-1 were designed outside the multiple cloning sites (MCS) in the vector and the resulting product size depends on the insert. **c** Quantitative real-time PCR analysis of *PoPDS* in systemically-infected *P. ostii* leaves. 18S-26S internal transcribed spacer (18S-26S-ITS) was used to normalize the transcript levels, and relative expression values were calculated compared with the highest expression value taken as 1.0 (untreated). Error bars represent ±SE of data from three independent experiments. The different letters indicate significant differences using Duncan's multiple range test at p 0.05.

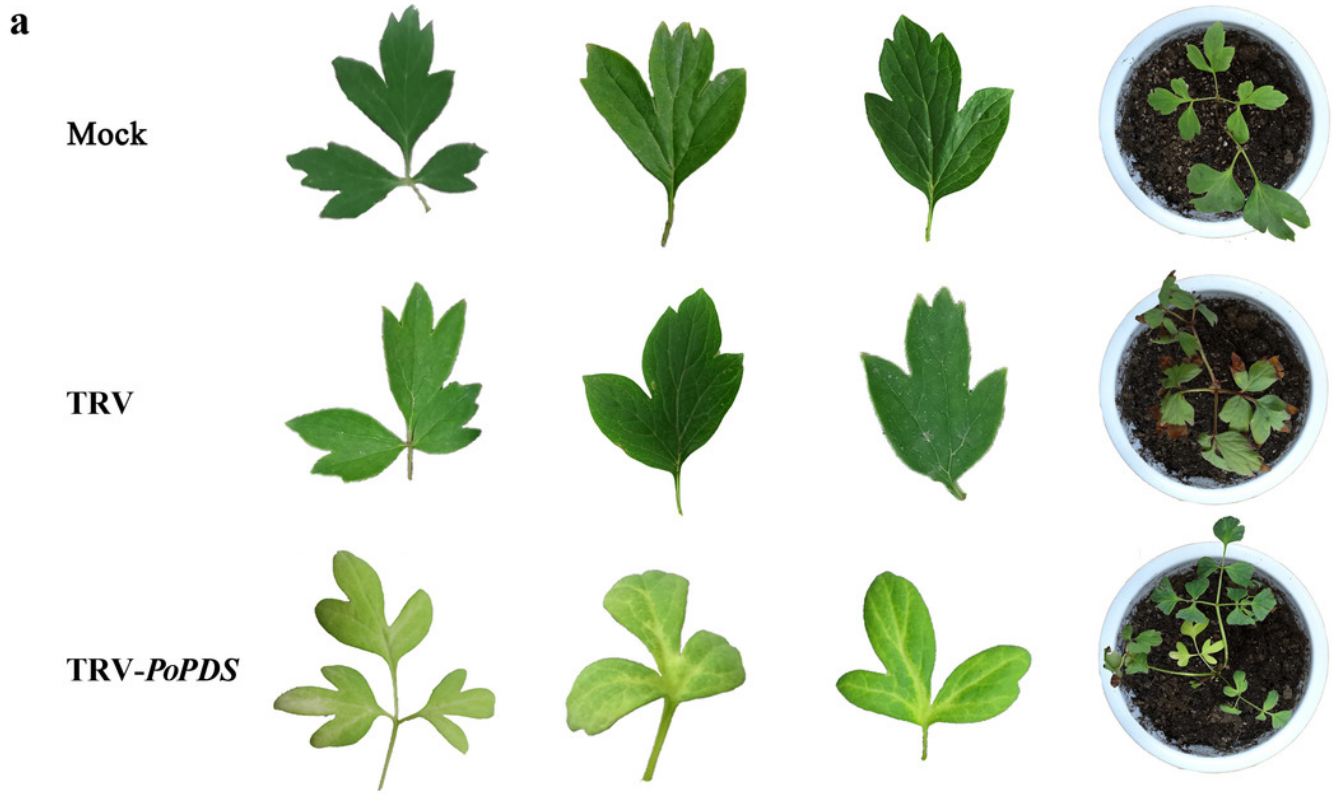
a
Mock
TRV
TRV-PoPDS
b
Mock
TRV
TRV-PoPDS
TRV1
TRV2-1
TRV2-2
18S-26S-ITS
c
Relative PoPDS expression
1.2
0.8
0.4
0
a
a
b
Mock
TRV
TRV-PoPDS

Figure 5

GFP expression in *P. ostii* leaves and roots inoculated with TRV-GFP

GFP fluorescence was observed under a laser scanning confocal microscope in *P. ostii* leaves (d-f) and roots (j-l) infected with TRV-GFP at 5 days post-infiltration (dpi). Fluorescence was not observed in leaves (a-c) and roots (g-i) of mock-treated plants. The cell outline (a, d, g, j), the dark fluorescence (b, e, h, k), and the combination photographed in bright field (c, f, i, l) are shown.

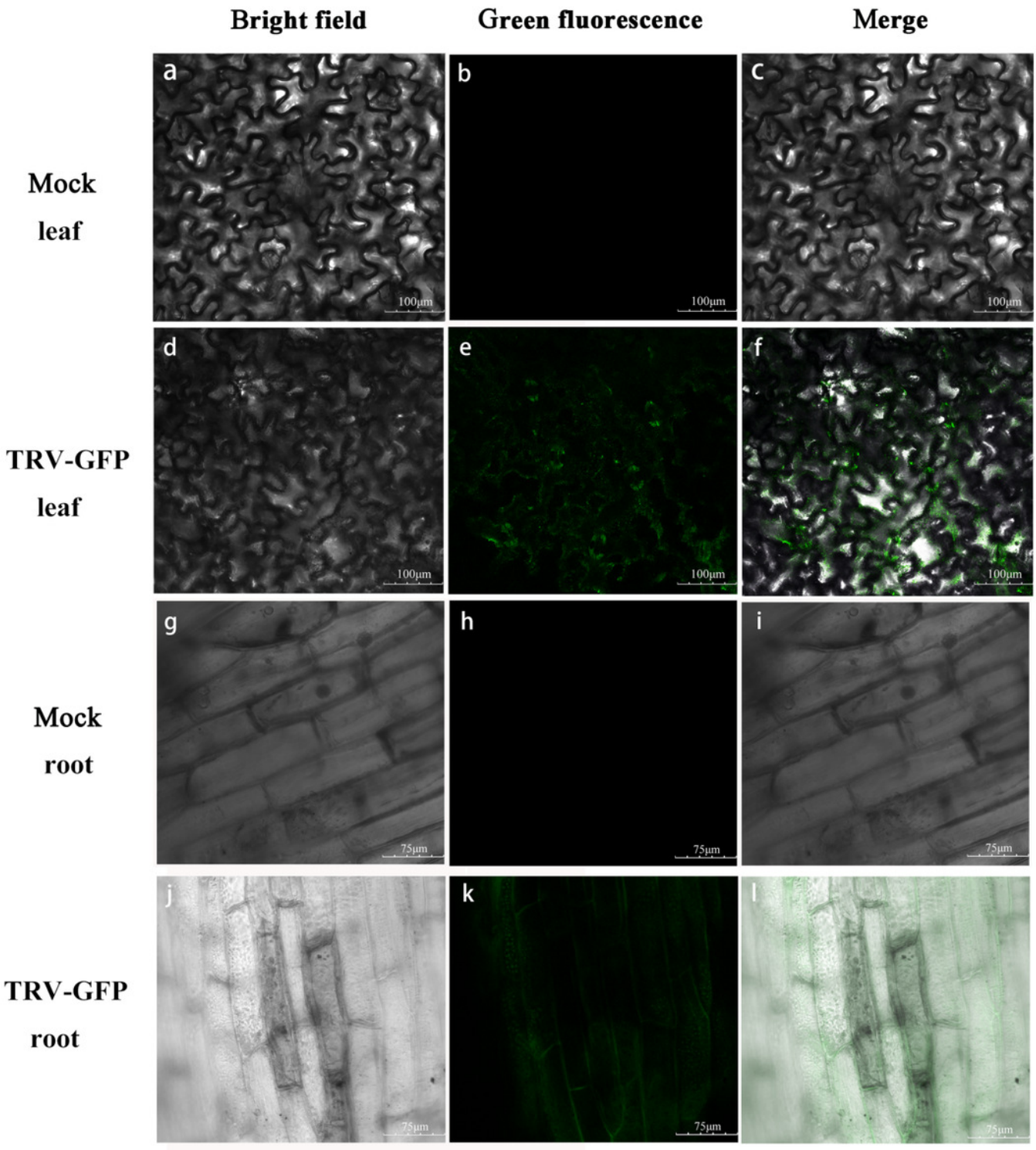
Bright field
Green fluorescence
Merge
Mock leaf
TRV-GFP leaf
Mock root
TRV-GFP root
a
b
c
d
e
f
g
h
i
j
k
l
100μm
75μm

Figure 6

Detection of GFP protein accumulation in TRV-GFP-inoculated *P. ostii* leaves and roots

a Western blot analysis of CP-GFP protein levels in mock treated, TRV-GFP-infected *P. ostii* leaves and roots at 5 days post inoculation. Ten micrograms of protein were loaded into each lane and an anti-GFP antibody was used to detect the CP-GFP fusion protein. Coomassie blue staining was used to confirm equal loading in each lane. **b** Semi-quantitative RT-PCR analysis of TRV1, TRV2, and GFP accumulation levels in mock treated, TRV-GFP-infected *P. ostii* leaves and roots. 18S-26S internal transcribed spacer (18S-26S-ITS) was used as internal control.

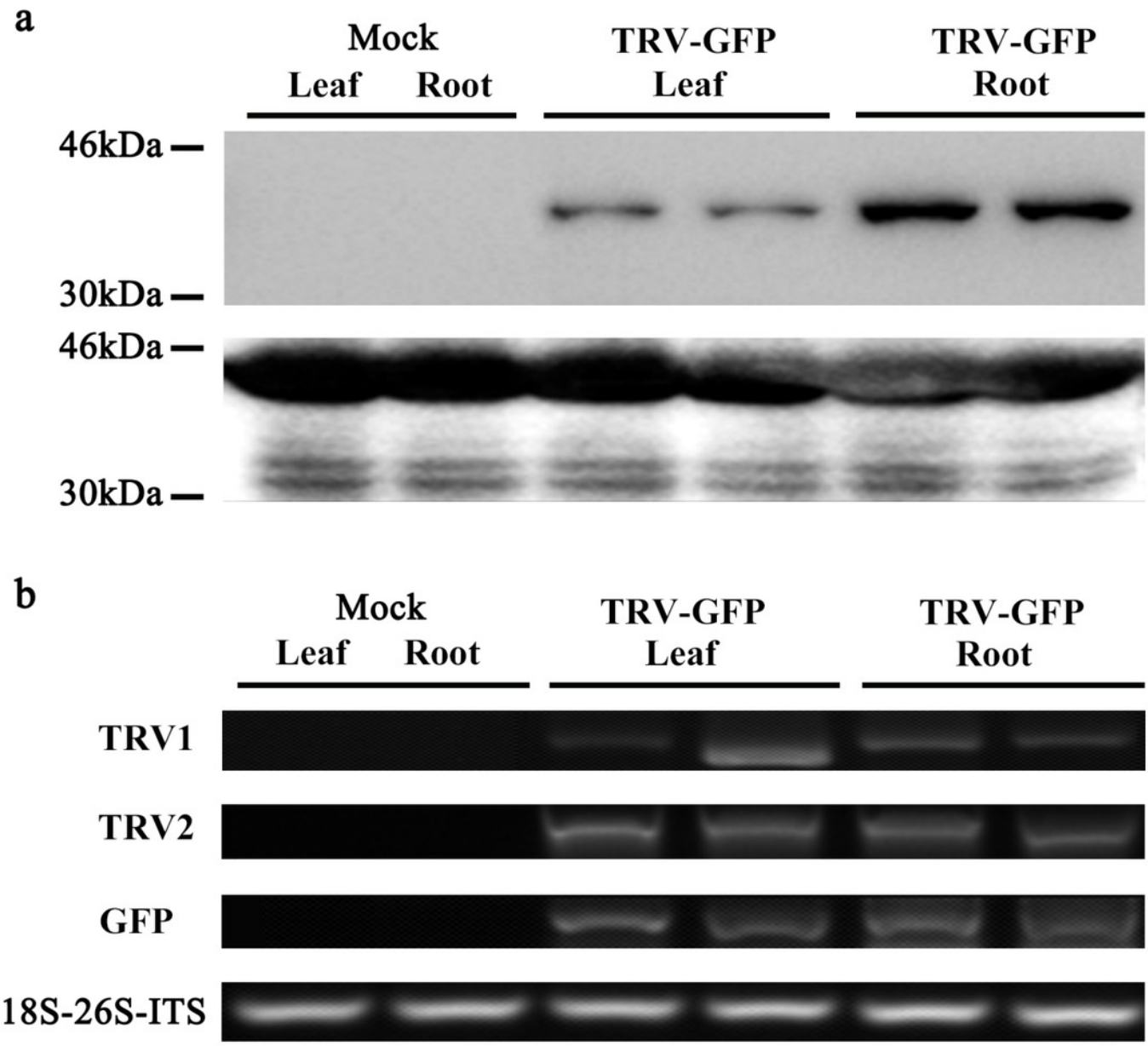
a
Mock
Leaf
Root
TRV-GFP
Leaf
TRV-GFP
Root
46kDa
30kDa
46kDa
30kDa
b
Mock
Leaf
Root
TRV-GFP
Leaf
TRV-GFP
Root
TRV1
TRV2
GFP
18S-26S-ITS